Journal of the
STRUCTURAL DIVISION
Proceedings of the American Society of Civil Engineers

REINFORCED CONCRETE RESPONSE TO SIMULATED EARTHQUAKES

By Toshikazu Takeda,[1] Mete A. Sozen[2] and N. Norby Nielsen,[3] Members, ASCE

INTRODUCTION

The response analysis of reinforced concrete structures subjected to strong earthquake motions requires a realistic conceptual model which recognizes the continually varying stiffness and energy-absorbing characteristics of the structure. Such a model is proposed in this paper and its applicability to reinforced concrete is tested experimentally with the use of specimens subjected to dynamic base motions.

University of Illinois Earthquake Simulator.—The University of Illinois Earthquake Simulator is an electro-hydraulic system (Fig. 1) comprising four main parts: (1) A hydraulic ram equipped with a servo-valve; (2) a power supply; (3) a command center; and (4) a test platform.

1. The hydraulic ram is rated at a peak capacity of 75,000 lb, a maximum velocity of 15 in. per sec, and a maximum double-amplitude displacement of 4 in. The servo-valve controls the ram motion through displacement signals transmitted by an LVDT mounted in the actuator assembly. The ram reacts against a steel pedestal prestressed to the test floor. The test floor provides a mass of approximately 4.5×10^6 lb.
2. The hydraulic power supply is provided by a variable-volume 120-hp pump with a flow capacity of 70 gpm.
3. The command center is equipped to receive three types of input: (a) Commands for periodic motion are generated by a low frequency oscillator;

Note.—Discussion open until May 1, 1971. To extend the closing date one month, a written request must be filed with the Executive Director, ASCE. This paper is part of the copyrighted Journal of the Structural Division, Proceedings of the American Society of Civil Engineers, Vol. 96, No. ST12, December, 1970. Manuscript was submitted for review for possible publication on March 3, 1970.

[1] Chf., Structural Section, Engineering Research Laboratory, Ohbayashi-Gumi Ltd., Tokyo, Japan.
[2] Prof. of Civ. Engrg., Univ. of Illinois, Urbana, Ill.
[3] Prof. of Civil Engrg., Univ. of Hawaii, Honolulu, Hawaii.

Journal of the Structural Division, 1970, 96(12): 2557-2573

(b) commands for programmed motion with periods longer than 1/60 of the test duration can be input by a function generator which translates arbitrary handdrawn wave forms into command signals; and (c) commands for earthquake simulation are input from magnetic tape in the form of displacement, velocity or acceleration versus time.

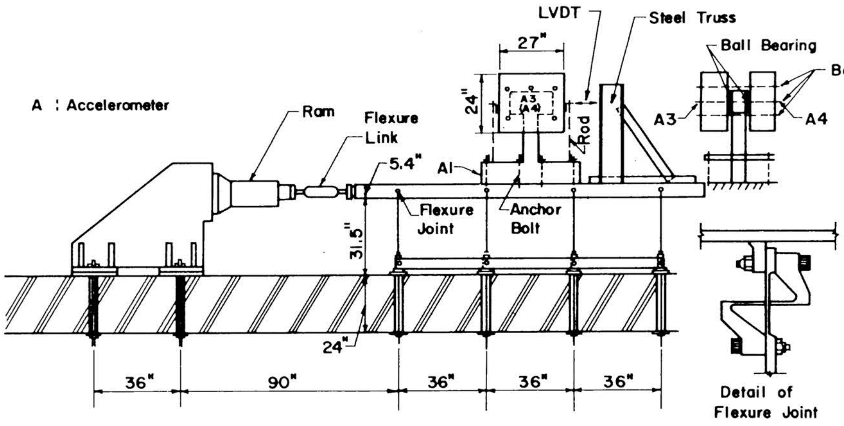

FIG. 1.—UNIV. OF ILLINOIS EARTHQUAKE SIMULATOR WITH TEST SPECIMEN IN PLACE

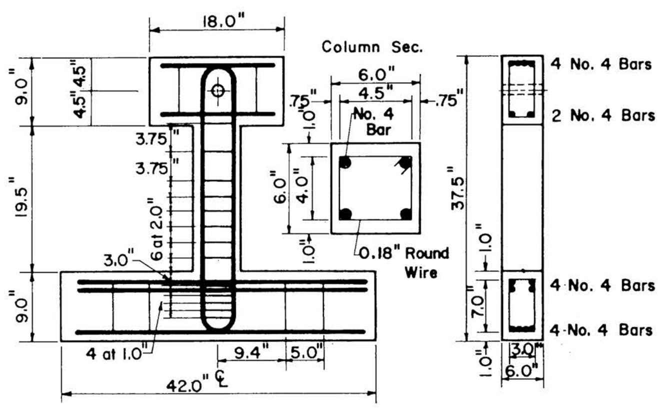

FIG. 2.—TEST SPECIMEN

4. The test platform is 12 ft by 12 ft in plan and comprises a 3/8-in. plate welded to 5-in. I-beams. It is supported by four series of flexure plates with a double-amplitude displacement limit of 5 in.

Test Specimen.—The test specimen is a simple, externally determinate structural unit which permits the investigation under dynamic conditions of the response of reinforced concrete members subjected to flexure. The diminsions and reinforcing arrangement are shown in Fig. 2. The static yield stress was 51,000 psi for the main reinforcement and 40,000 psi for the transverse reinforcement. Five specimens were tested with concrete properties at the time of test as follows:

	T1	T2	T3	T4	T5
Compressive strength, in pounds per square inch	4,020	4,480	4,830	4,400	4,280
Tensile (splitting) strength, in pounds per square inch	350	400	420	340	320

As shown in Fig. 1, two steel masses of 2,015 lb were hung on each side of the specimen on a 1-in. steel shaft resting on ball bearings. To restrain large rotations of the steel mass, two 0.25-in. round prestressed rods tied the mass to the platform (Fig. 1).

Test Procedures.--Specimens T3 and T4 were tested statically. An alternating lateral load was applied at the level of the steel shaft supporting the mass. In addition to the load, deflections and reinforcement strains were measured.

Specimen T1 was subjected to periodic base motions while specimens T2 and T5 were subjected to simulated earthquake motions. In these tests, continuous records of base and mass accelerations, mass displacement, and reinforcement strains were obtained.

STATIC RESPONSE

The hysteresis loops defined by the principles for constructing the static force-displacement relationship are critical to the success of the dynamic analysis. Therefore, the variations which occur in this relationship with load level and history should be considered in detail.

The static response was idealized by defining a primary curve for initial loading and a set of rules for reversals as described in the next two sections.

Primary Curve.—Three linear segments in each quadrant define the primary curve [Fig. 3(*a*)]. The first break in the curve refers to cracking. The coordinates of this point (P_{cr}, D_{cr}) were computed routinely with the concrete flexural tensile strength assumed to be 530 psi.

The yield load, P_y, was obtained assuming a parabolic compressive stress-strain curve for the concrete. The yield deflection, D_y, was the sum of four parts: (1) Deflection caused by curvature based on cracked section; (2) deflection caused by slip of the reinforcement and depression of the concrete at the beam-column interface; (3) deflection caused by deformation of the test platform; and (4) the shearing deflection. To determine part 2, it was assumed that the anchorage bond at yielding of the bar extended uniformly over 20 bar diam. The depression of the concrete was calculated by treating the horizontal beam as a semi-infinite plate (2) loaded by a linearly varying stress corresponding to the stress distribution in the concrete at the interface. The rotation was determined by considering the depression at the centroid of the stress block. Part 3, a feature peculiar to the test setup, was obtained from measurements made during the static tests. The relative contributions of the four parts to the total deflection were: part 1, 56 %; part 2, 31 %; part 3, 11 %; part 4, 2 %. In many applications, part 2, which is usually ignored, may exceed part 1.

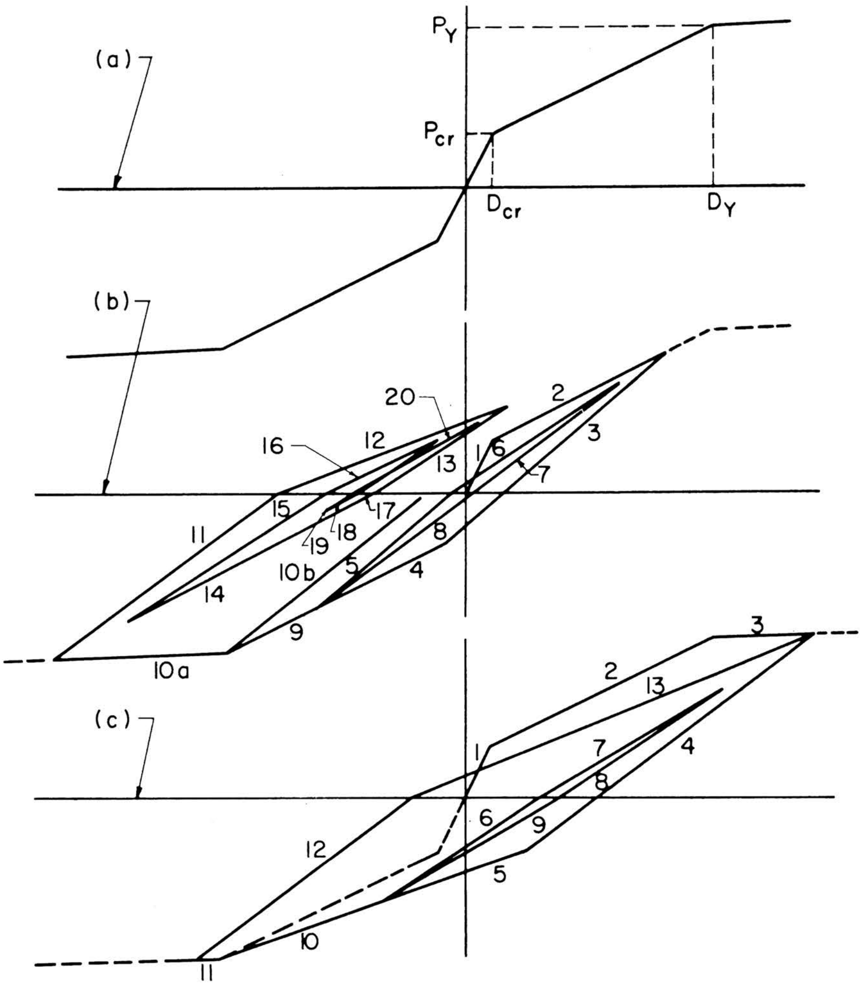

FIG. 3.—EXAMPLES OF ASSUMED STATIC LOAD-DEFLECTION RELATIONSHIP

The slope of the third segment of the primary curve was related to the strain-hardening properties of the reinforcement. The deflection caused by bending at a steel stress equal to 80 % of the steel strength, f_s' was calculated using a bilinear moment-curvature relationship. The total deflection at that stress was assumed to be D_y multiplied by the ratio of the bending deflection at $0.8f_s'$ to the bending deflection at yield.

The following material properties were assumed in determining the primary curve: (1) Compressive strength of the concrete, 4,400 psi; (2) modulus of rupture for the concrete, 530 psi; (3) Young's modulus for the concrete: 3.6×10^6 psi; (4) Young's modulus for the steel, 29×10^6 psi; and (5) yield stress for the steel, 51,000 psi.

Response Under Load Reversals.—In the following paragraphs, a series of rules are stated for constructing the load-deflection curve corresponding to load reversals. Because there are many possible alternatives at each point in the loading history, it is not convenient to provide a continuous description of the load-deflection curve. Rules are given for loading and unloading for different conditions and shown in Figs. 3(*b*) and 3(*c*).

1. Condition—The cracking load, P_{cr}, has not been exceeded in one direction. The load is reversed from a load P in the other direction. The load P is smaller than the yield load P_y.

Rule—Unloading follows a straight line from the position at load P to the point representing the cracking load in the other direction.

Example--Segment 3 in Fig. 3(*b*) (If unloading occurs before deformations represented by segment 2, the rules provide no hysteresis loop.)

2. Condition—A load P_1 is reached in one direction on the primary curve such that P_1 is larger than P_{cr} but smaller than the yield load, P_y. The load is then reversed to $-P_2$ such that $P_2 < P_1$.

Rule—Unload parallel to loading curve for that half cycle.

Example--Segment 5 parallel to segment 3 in Fig. 3(*b*).

3. Condition—A load P_1 is reached in one direction such that P_1 is larger than P_{cr} but not larger than the yield load, P_y. The load is then reversed to $-P_3$ such that $P_3 > P_1$.

Rule—Unloading follows a straight line joining the point of return and the point representing cracking in the other direction.

Example—Segment 10(*b*) in Fig. 3(*b*).

4. Condition—One or more loading cycles have occurred. The load is zero.

Rule—To construct the loading curve, connect the point at zero load to the point reached in the previous cycle, if that point lies on the primary curve or on a line aimed at a point on the primary curve. If the previous loading cycle contains no such point, go to the preceding cycle and continue the process until such a point is found. Then connect that point to the point at zero load.

Exception—If the yield point has not been exceeded and if the point at zero load is not located within the horizontal projection of the primary curve for that direction of loading, connect the point at zero load to the yield point to obtain the loading slope.

Examples—Segment 12 in Fig. 3(*b*) represents the exception. It is aimed at the yield point rather than at the highest point on segment 2. Segment 8 in Fig. 3(*b*) represents a routine application, while segment 20 represents a case where the loading curve is aimed at the maximum point of segment 12.

5. Condition—The yield load, P_y, is exceeded in one direction.

Rule—Unloading curve follows the slope given by the following equation adapted from Ref. 1:

$$k_r = k_y \left(\frac{D_y}{D}\right)^{0.4} \qquad (1)$$

in which k_r = slope of unloading curve; k_y = slope of a line joining the yield

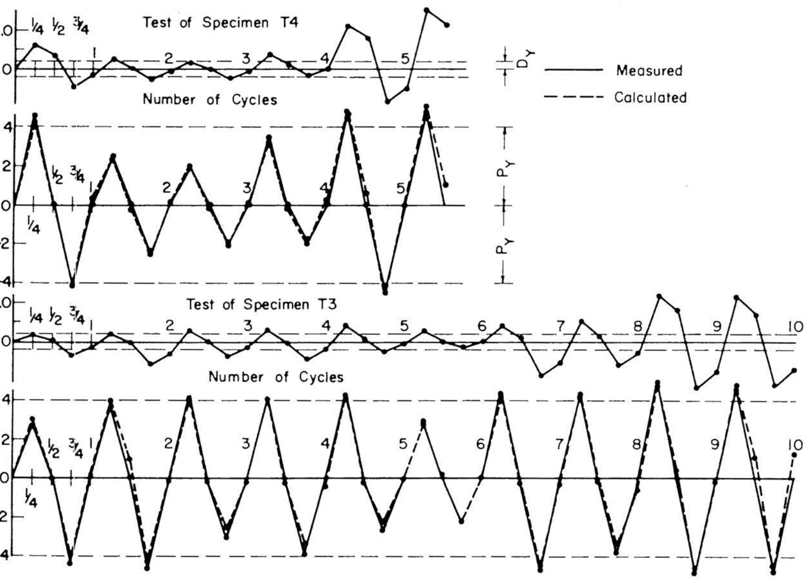

FIG. 4.—MEASURED AND CALCULATED STATIC RESPONSE

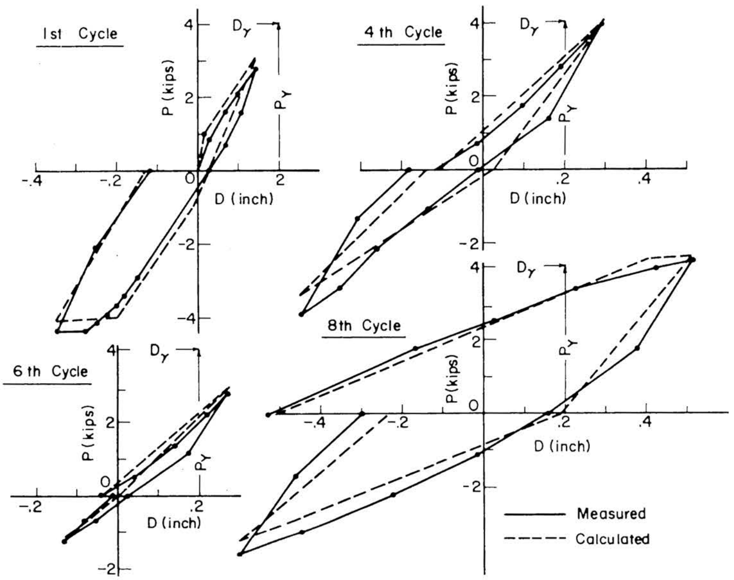

FIG. 5.—MEASURED AND CALCULATED HYSTERESIS LOOPS FOR STATIC LOADING

TABLE 1.—MEASURED AND CALCULATED RESPONSE TO PERIODIC BASE MOTIONS

Response (1)	ALTERNATING ACCELERATION PULSES: Frequency, in cycles per second (2)	Acceleration: Maximum, in g (3)	Acceleration: Steady state average, in g (4)	Displacement: Maximum, in inches (5)	Displacement: Steady state average, in inches (6)	SINUSOIDAL MOTION: Frequency, in cycles per second (7)	Acceleration: Maximum, in g (8)	Acceleration: Steady state average, in g (9)	Displacement: Maximum, in inches (10)	Displacement: Steady state average, in inches (11)
Base motion	8	4.5	4.1	0.26	0.25	4	1.73	0.87	0.61	0.54
Measured response		1.32	0.92	0.74	0.43		1.25	1.09	1.15	1.07
Calculated response										
h = 0		1.07	0.77	0.77	0.39		1.25	1.02	1.25	1.07
h = 0.02		1.22	0.91	0.65	0.39		1.23	1.14	1.15	1.05

NOTE: Mass accelerations are average values of accelerations measured on north and south sides of mass.

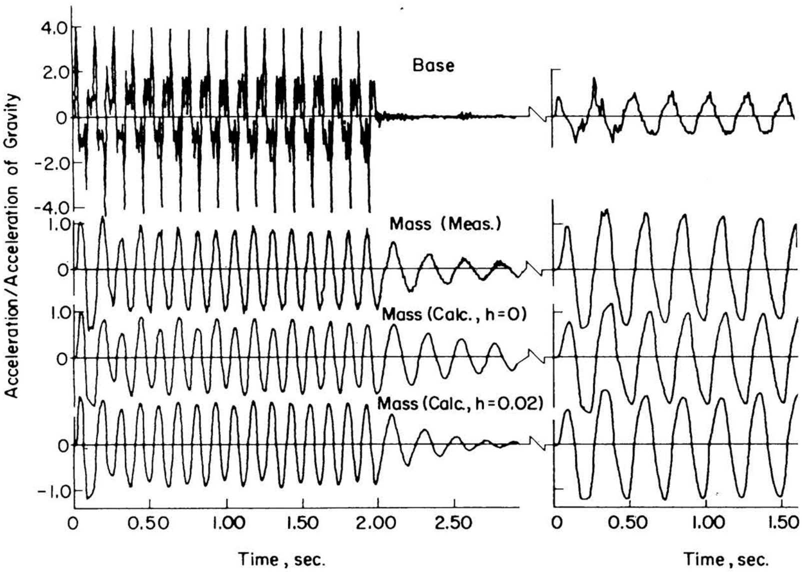

FIG. 6.—MEASURED AND CALCULATED ACCELERATION RESPONSE TO PERIODIC BASE MOTIONS

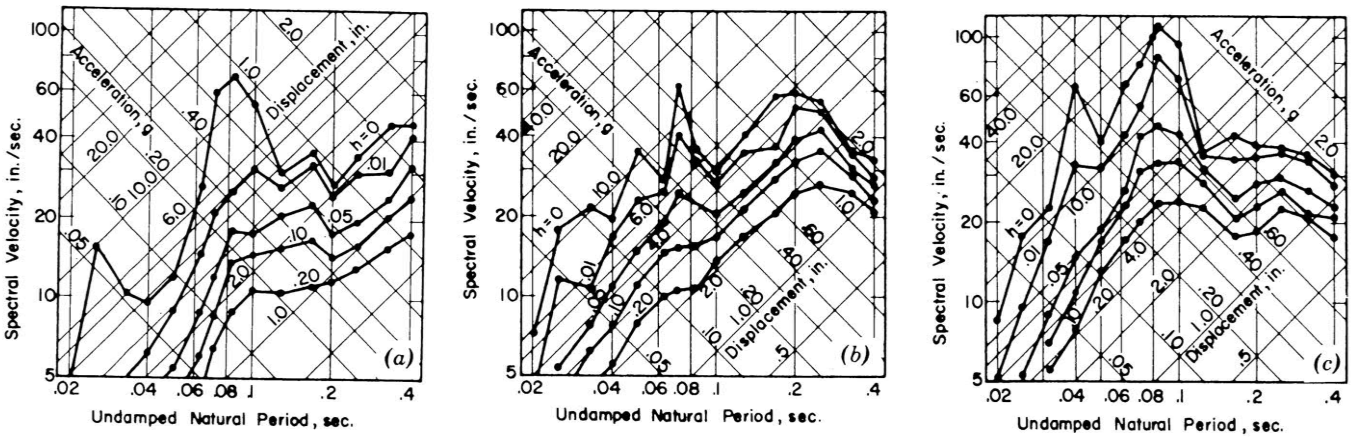

FIG. 7.—SPECTRAL RESPONSE: (*a*) RUN 11; (*b*) RUN 12; (*c*) RUN 21

point in one direction to the cracking point in the other direction; D = maximum deflection attained in the direction of the loading; and D_y = deflection at yield.

Example: Segment 4 in Fig. 3(*c*).

6. Condition: The yield load is exceeded in one direction but the cracking load is not exceeded in the opposite direction.

Rule—Unloading follows Rule 5. Loading in the other direction continues as an extension of the unloading line up to the cracking load. Then, the loading curve is aimed at the yield point.

Example--Segments 4 and 5 in Fig. 3(*c*).

7. Condition—One or more loading cycles have occurred.

Rule—If the immediately preceding quarter-cycle remained on one side of the zero-load axis, unload at the rate based on rules 2, 3, and 5, whichever

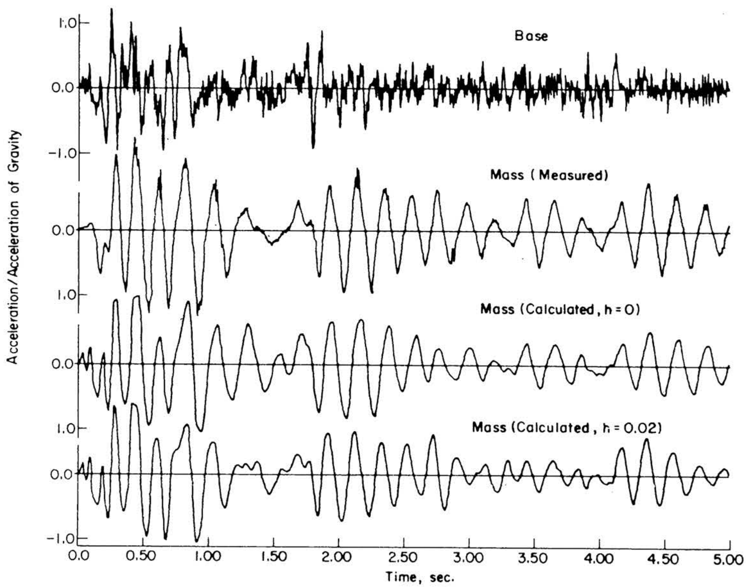

FIG. 8.—MEASURED AND CALCULATED ACCELERATION RESPONSE TO RUN 11

governed in the previous loading history. If the immediately preceding quarter-cycle crossed the zero-load axis, unload at 70 % of the rate based on rules 2, 3, or 5, whichever governed in the previous loading history, but not at a slope flatter than the immediately preceding loading slope.

Example--Segment 7 in Fig. 3(*b*).

Comparison of Calculated and Measured Static Response Curves.—Specimens T3 and T4 were subjected to a program of alternating deflections comparable to those measured in the dynamic tests. The measured and calculated loads are compared in Fig. 4. Several measured and calculated static hysteresis loops are shown in Fig. 5. The results of these two tests indicated that the set of rules adopted for defining the static response were satisfactory in predicting the maximum loads and in delineating the hysteresis loops.

Test specimen T3 was subjected to a program of deflections through 10 cycles. The magnitudes of the deflection in the first eight cycles were comparable to those measured in the earthquake-simulation test. The solid curve in Fig. 4 shows the deflections reached and the loads generated at each cycle. The broken curve indicates the loads calculated according to the set of rules described in the previous sections. The comparison of the maximum loads is satisfactory.

Load-deflection curves for four individual cycles are shown in Fig. 5. The loops do not coincide in every case. However, the area contained in the loop is nearly the same for the calculated and measured loops.

RESPONSE TO PERIODIC BASE MOTIONS

Specimen T1 was subjected to a series of alternating acceleration pulses at 8 cps followed, after a pause, by a sinusoidal motion at 4 cps (Fig. 6). These tests were made to study the response of the specimen at high levels of excitation. The base-motion frequencies were chosen to be close to the calculated natural frequency in the first case and to the frequency observed at the end of the first test in the second case. The natural frequency was calculated on the basis of a force-deflection rate obtained by joining the origin in Fig. 3(*a*) to the yield point by a straight line.

In general, the agreement of the calculated and measured acceleration response curves was good (Fig. 6 and Table 1) indicating that the method of analysis used can be applied in ranges where the mass displacement is on the order of six times the initial yield deflection, a range achieved during the test with the sinusoidal base motion. The specimen survived the initial test with the alternating acceleration pulses at a displacement of less than four times the yield deflection although the base motion was close to the initial natural frequency of the system. The reason for this is an intrinsic characteristic of the reinforced concrete specimen; as soon as the high excitation was initiated, the stiffness of the specimen changed.

The observed frequency after the first test was 4 cps (based on relatively high-amplitude vibration after the base motion was stopped.) It was 2.5 cps after the second test. It is evident that to trace the response of the system analytically through a program of strong excitation, it is essential to assume a decaying stiffness in a realistic analysis. The maximum measured response of 1.32 g is high in comparison with the maximum static force of 1.1 g developed at a comparable deflection. The measured strain rate for the steel approached the order 0.1 per sec, a rate which could increase the yield stress by 10 ksi.

SIMULATED EARTHQUAKE MOTIONS

Three tests were run with the motion of the platform designed to simulate various earthquake motions. The main characteristics of the platform motions are described in the following sections.

Run 11: In run 11, the displacement record for the N-S component of the El Centro 1940 earthquake was fed into the command center of the actuator such that 40 sec of the original earthquake record were played through in 5 sec. The maximum platform acceleration was measured to be 1.28 g and the maximum platform displacement was 1.2 in. The measured platform acceler-

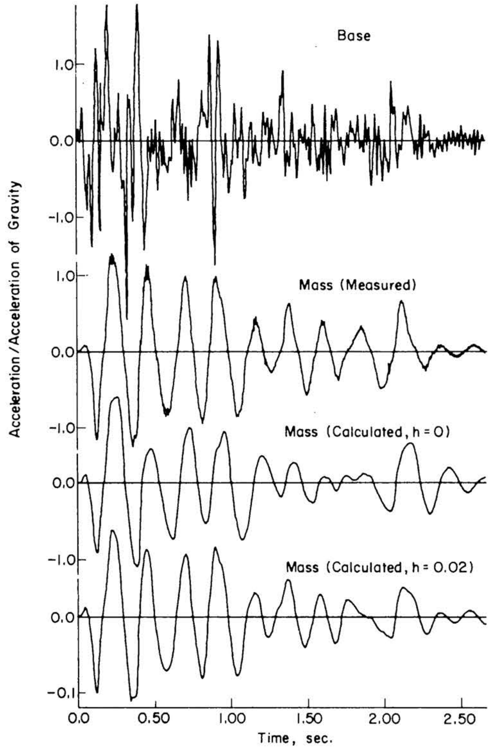

FIG. 9.—MEASURED AND CALCULATED ACCELERATION RESPONSE TO RUN 12

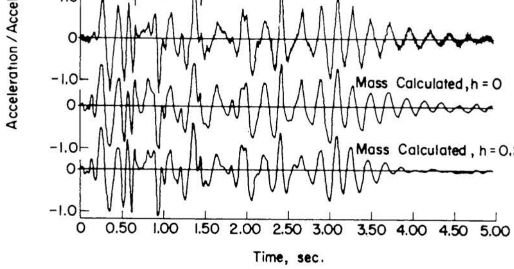

FIG. 10.—MEASURED AND CALCULATED ACCELERATION RESPONSE TO RUN 21

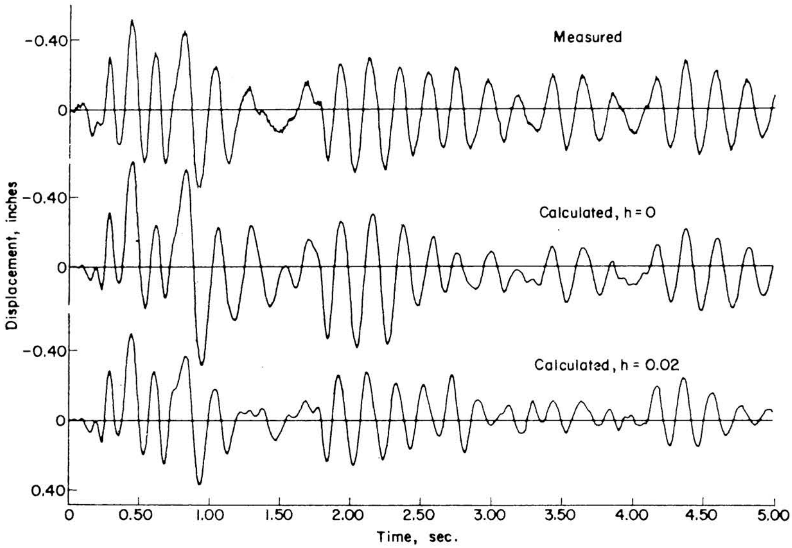

FIG. 11.—MEASURED AND CALCULATED MASS DISPLACEMENT IN RUN 11

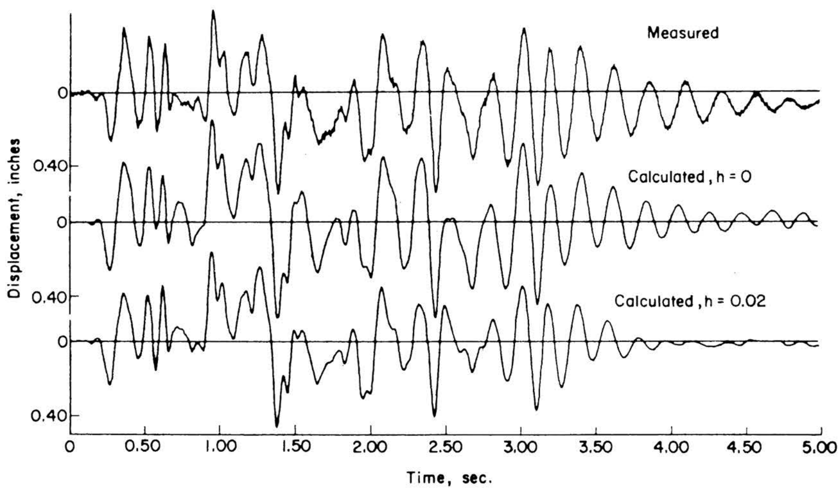

FIG. 12.—MEASURED AND CALCULATED MASS DISPLACEMENT IN RUN 12

ation is shown in Fig. 8. The response spectrum of the platform motion is shown in Fig. 7(*a*).

In general, the acceleration record resembles qualitatively the original record measured at El Centro. Three major disturbance zones are discernible in the record: the first one at the beginning of the earthquake, the second one at 1.7 sec (platform time), and the third at 3.8 sec.

For the intended conditions of modeling, to get an ideal correlation between the response spectra for the platform earthquake and the real earthquake, it is necessary that the platform accelerations be eight times the earthquake

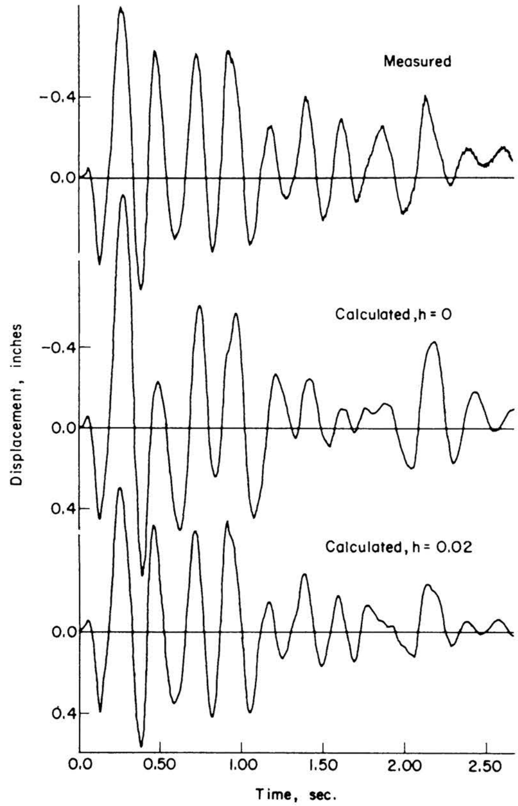

FIG. 13.—MEASURED AND CALCULATED MASS DISPLACEMENT IN RUN 21

accelerations if the platform time is one-eighth of the earthquake time. Furthermore, the number of zero crossings per second of the acceleration record on the platform should be eight times that observed in the original record. Run 11 and the following runs 12 and 21 did not satisfy these requirements. However, if the test specimen remains in the flat response range for velocity, it suffices to have the platform velocity comparable to the earthquake-motion velocity. Thus, while the spectral response for the platform does not correlate with that for the full scale earthquake at periods below 0.1 sec (platform time), it does present a satisfactory correlation at longer periods.

Run 12: In this run, the original El Centro 1940 N-S tape was compressed 16 times resulting in a maximum acceleration of 2.4 g. The maximum displacement was 0.88 in. The platform acceleration record is shown in Fig. 9 and the response spectra in Fig. 7(*b*).

The overall characteristics of the spectral response for run 12 are similar to those of run 11. In comparing the two, the natural periods in run 11 should be divided by two and the accelerations should be doubled.

Run 21: This run was patterned after the N21E component of Taft 1952. The time was compressed by a factor of 10 while the maximum acceleration

TABLE 2.—MEASURED AND CALCULATED RESPONSE TO SIMULATED EARTHQUAKE MOTIONS

Response	RUN 11 (TEST SPECIMEN T2)				RUN 12 (TEST SPECIMEN T2)				RUN 21 (TEST SPECIMEN T5)			
	Acceleration		Displacement		Acceleration		Displacement		Acceleration		Displacement	
	East, in *g*	West, in *g*	East, in inches	West, in inches	East, in *g*	West, in *g*	East, in inches	West, in inches	East, in *g*	West, in *g*	East, in inches	West, in inches
(1)	(2)	(3)	(4)	(5)	(6)	(7)	(8)	(9)	(10)	(11)	(12)	(13)
Base motion	1.28	1.00	0.14	1.17	1.97	2.40	0.11	0.88	2.7	2.6	1.70	0.64
Measured response												
North	1.35	1.25			1.28	1.22			1.30	1.37		
South	1.27	1.33			1.28	1.28			1.28	1.35		
Average	1.31	1.29	0.46	0.52	1.28	1.25	0.54	0.84	1.29	1.36	0.44	0.54
Calculated response												
$h = 0$	1.07	1.04	0.57	0.61	1.15	1.10	0.73	1.14	1.06	1.03	0.55	0.52
$h = 0.02$	1.09	1.07	0.34	0.49	1.17	1.12	0.56	0.71	1.16	1.13	0.48	0.46

NOTE: Mass accelerations measured by accelerometers mounted on north and south sides of mass.

was increased to 2.7 g (Fig. 10). The calculated spectral response is shown in Fig. 7(*c*).

RESPONSE TO SIMULATED EARTHQUAKE MOTIONS

The measured accelerations and displacements of the mass attached to the specimen in test runs 11, 12, and 21 are shown in Figs. 8 through 13. Maximum values are summarized in Table 2.

Acceleration measurements were made on both the north and south faces of the mass. These measurements differed by very small amounts, indicating that the torsion of the mass was negligible.

The mass response in runs 11 and 21 had different characteristics. The maximum response occurred at the beginning of the simulated earthquake in run 21. High accelerations were observed periodically throughout the test. In run 11, there were three reasonably distinct zones of high excitation in the mass response as in the platform motion.

The decay in the stiffness of the test specimen was indirectly indicated by the variations in the average number of zero-crossings of the acceleration record throughout the individual runs. In run 11 the mean zero-crossing rate decreased from 10.5 per sec at the beginning of the earthquake motion to 8.6 per sec at the end. In run 12, the apparent decay of the stiffness was less. The zero-crossing rate varied from 8.5 per sec at the beginning of the motion to 8.0 per sec at the end. In run 21, zero-crossings per second decreased from 14 at the beginning of the earthquake to nine at the end.

In general, the response varied from cycle to cycle throughout the earthquake, indicating the availability of a considerable amount of energy absorption. The yield force was exceeded in both directions three times in run 11, twice in run 12, and four times in run 21. Initial yield deflection was exceeded in both directions approximately twelve times in run 11, six times in run 12 and twelve times in run 21. In runs 11 and 21, the maximum displacement was approximately 2.6 times the initial yield deflection. In run 12, the maximum displacement was 4.2 times the initial yield deflection. In each run, the number of excursions beyond the yield deflection was greater than the number of excursions beyond the yield load, another indication of the reduction in the stiffness of the system. Examination of the specimen after runs 11 and 21 indicated the presence of fine flexural cracks at the joint between the member and the horizontal base beam. Strain measurements on the reinforcement at the same location indicated that yielding of the reinforcement had occurred. After run 12, inclined cracks were observed on the surface of the specimen but the widths of these cracks were less than 0.05 in. and did not indicate distress in shear.

CALCULATED RESPONSE TO SIMULATED EARTHQUAKE MOTIONS

The response at the centroid of the mass to the simulated earthquake motions was calculated using a step-by-step numerical integration method. The acceleration was assumed to vary linearly over intervals of 0.002 sec while the integration step was 0.0004 sec. The static force-deflection relationship of the reinforced concrete specimen was programmed in accordance with the rules described earlier in the paper. Run 12 was conducted with specimen T2 after the same specimen had already been subjected to run 11. In the analysis, runs 11 and 12 were treated continuously. However, after the base motion for run 11 was terminated, the acceleration and the velocity of the mass were made zero.

The response was calculated for no damping and for an equivalent viscous damping equal to 2 % of the critical (Figs. 8-13). The main effect of the assumed damping was on the calculated displacements.

In general, the measured and calculated response histories compared very favorably. The measured maximum accelerations exceeded the calculated values (Table 2). The measured strain rate in the reinforcement approached 0.1 per sec, a rate which would justify an increase in the steel yield stress, and therefore in the calculated acceleration, by 20 %. Maximum displacements calculated for h = 0.02 compared better with the measured values than those based on zero damping. After the base motion was terminated, the small-amplitude vibration of the specimens was represented better by calculations based on zero damping.

CONCLUSIONS

1. The stiffness and energy-absorbing capacity of the reinforced concrete test specimens changed considerably and, at certain times, very rapidly throughout the duration of the simulated earthquake.

2. A realistic conceptual model for predicting the dynamic response of a reinforced concrete system should be based on a static force-displacement relationship which reflects the changes in stiffness for loading and unloading as a function of the previous loading history.

3. Dynamic response calculated on the basis of the proposed force-displacement relationship resulted in satisfactory agreement with the measured response at all levels of excitation during the tests with periodic and earthquake motions.

4. With the hysteresis loops defined by the proposed force-displacement relationship, it was not necessary to invoke additional sources of energy absorption for a satisfactory prediction of the dynamic response.

ACKNOWLEDGMENTS

The University of Illinois Earthquake Simulator was acquired under equipment grant GK 980 by the U.S. National Science Foundation. The reported work was carried out at the Structural Research Laboratory of the University of Illinois under NSF research grant GK 1118X.

T. Takeda participated in the project while on a fellowship awarded by Ohbayashi-Gumi Construction Co., Osaka, Japan. Acknowledgment is due V. J. McDonald, Associate Prof. of Civil Engineering, and P. Gulkan, F. Imbeault, E. Perry and S. Otani, for their contributions to the execution and analysis of the tests.

APPENDIX I.—REFERENCES

---

1. Timoshenko, S., and Goodier, J. N., *Theory of Elasticity*, McGraw-Hill Book Co., Inc., New York, 1951, p. 96.
2. Takeda, T., "Study of the Load-Deflection Characteristics of Reinforced Concrete Beams Subjected to Alternating Loads [in Japanese]," *Transactions*, Architectural Institute of Japan, Vol. 76, Sept., 1962.

APPENDIX II.—NOTATION

The following symbols are used in this paper:

D = maximum deflection attained in direction of loading;
D_{cr} = deflection at cracking;
D_y = deflection at yield;
k_r = slope of unloading curve;
k_y = slope of line joining the yield point in one direction to the cracking point in the other direction;
P_{cr} = load at cracking;
P_y = load at yield; and
P_1, P_2, P_3 = loads.